Title: On the Link Between Ozone Depletion and Global Warming

Authors: Peter L. Ward[1]*†

Affiliations:

[1] U.S. Geological Survey, retired, Teton Tectonics, P.O. Box 4875, Jackson, WY 83001, USA.

* Correspondence to: E-mail: peward@wyoming.com

† Website: www.ozonedepletiontheory.info

[Website will be made public when paper is published. Reviewers can see it at www.ozonedepletiontheory.info/ozonemain/   User: jackson Password: wyoming]

Abstract: Global warming increased substantially as emissions of anthropogenic chlorofluorocarbons began to increase in 1970, depleting stratospheric ozone. Warming leveled off in 1998 when chlorofluorocarbon emissions and ozone depletion stopped increasing. Ozone depletion allows more high-energy ultraviolet-B radiation to reach Earth's surface. Ozone is also depleted by chlorine and bromine gases emitted by volcanoes. Major explosive volcanoes deplete ozone but form sulfuric-acid aerosols in the lower stratosphere, reflecting and dispersing sunlight, causing net cooling. Effusive basaltic volcanoes deplete ozone but do not form aerosols, causing net warming. Ozone depletion heats Earth far more effectively than greenhouse gases because, according to Planck, energy in radiation is proportional to frequency, not bandwidth as currently assumed. Ultraviolet-B contains ~48 times the energy of infrared radiation absorbed by greenhouse gases.

One Sentence Summary: Ozone depletion caused by anthropogenic chlorofluorocarbons and volcanoes appears far more important for global warming than currently calculated.

Main Text:
    Average temperatures at Earth's surface result from a balance between thermal energy received from the sun and thermal energy lost from Earth's surface through convection into the atmosphere and radiation into space. Greenhouse gas theory explains global warming by greenhouse gases absorbing terrestrial radiation, inhibiting energy losses from Earth. Ozone depletion theory, described in this paper, explains global warming by an increase in how much solar energy reaches Earth's surface due to an observed decrease in the optical thickness of the ozone layer. Solar radiation is much hotter – contains much more energy – than terrestrial radiation.

    Ozone is continuously created and destroyed in Earth's atmosphere, forming a layer primarily between 15 and 35 km above Earth's surface with a concentration of no more than 8 parts per million. It is well known that life as we know it on Earth would not survive if the ozone layer did not absorb much of the highest energy ultraviolet-B solar radiation that causes sunburn, skin cancer, and, in sufficient amounts, mutations. Since the thermal energy contained in radiation is equal to frequency times the Planck constant

(*1*), the thermal energy in ultraviolet-B is ~48 times the energy in infrared radiation absorbed most strongly by greenhouse gases. Net thermal energy is directly proportional to the fourth power of thermodynamic temperature (Stefan-Boltzmann law).

The highest-energy components of solar radiation (>10 eV, electron volts) are absorbed typically above 85 km in the atmosphere where they cause photoionization maintaining the ionosphere. Energies around 5 eV (Fig. 1, green bar), that split molecular oxygen leading to the formation of ozone, are mostly absorbed above the tropopause (9 to 17 km above Earth) because the atmosphere contains more than enough oxygen to absorb all the radiation available to dissociate it. Energies above 4 eV (orange bar) that destroy ozone are absorbed typically before reaching the tropopause in an endless photochemical cycle known as the Chapman cycle (*2*) that creates and destroys ozone, warming the stratosphere. When the normal amount of ozone in the ozone layer is depleted, more ultraviolet-B energy (red shaded area) reaches Earth, cooling the stratosphere and increasing evaporation and air temperatures over land. Most importantly, the increased ultraviolet-B radiation adds heat efficiently to the oceans, covering 71% of Earth, by penetrating tens of meters below the ocean surface (*3*). Because the ocean stores most of the heat in Earth's climate system, warming the ocean produces long-term global warming.

Between 1978 and 2008, ultraviolet-B radiation with wavelengths close to 305 nanometers (983 terahertz, 4.1 eV) was observed at the Earth's surface to increase 23% at 50^oS, 9% at 35^oS, 7% at 39^oN, 9% at 50^oN (*4*).

Ozone accumulates above polar regions during winter (Fig. S1), warming the lower stratosphere and causing unusually cold temperatures at Earth's surface. This accumulation of ozone has been observed during late winter and early spring to be depleted by as much as 50% relative to concentrations during the same months in the 1960s (*5*). Increased depletion increases the amount of ultraviolet-B radiation reaching Earth, primarily warming daily minimum temperatures. The largest warming trend in the world observed since the 1960s has been under the northern parts of the Antarctic ozone hole in late winter and early spring, observed most clearly along the Antarctic Peninsula (*6-8*).

Ozone is depleted primarily by chlorine and bromine emitted in gases manufactured by humans, emitted by erupting volcanoes, and even emitted by quietly degassing volcanoes (*9*). Because of the catalytic nature of the Chapman cycle, one chlorine atom can destroy 100,000 molecules of ozone (*10*).

Ozone Depletion and Volcanoes
Total column ozone, the amount of ozone in a vertical column above a point on Earth, varies by the minute, time of day, season, and latitude (*11*). But annual averages at each station tend to be similar and it is these averages that relate most directly to annual average surface temperatures.

The longest continuous measurements of total column ozone have been made since 1927 at Arosa, Switzerland (black line, Fig. 2) (*12*). The dashed grey line with blue data markers shows, for 1964 to 2009, the annual mean area-weighted total ozone deviation from the 1964 to 1980 means for northern mid-latitudes (30-60°N) scaled from -8% at the

bottom of the figure to 10% at the top (*13*). Years of increasing or decreasing ozone are nearly identical at Arosa and for this area-weighted mean with small differences in amplitude. Thus the Arosa data provide a reasonable approximation for annual mean total column ozone throughout northern mid-latitudes since 1927.

Ozone at Arosa averaged 331 DU (Dobson units) until 1974, fell 9.4% to 300 DU by 1993 and began generally rising again until 2011. The long-term decrease in ozone has been reliably associated with an increase in the concentration of anthropogenic tropospheric chlorine (green line, y-axis inverted) through chlorine catalyzed destruction of ozone (*14*). Discovery of the ozone hole over Antarctica in 1984 (*15*) galvanized interest in negotiating the Montreal Protocol on Substances That Deplete the Ozone Layer first signed in 1987. Under this protocol, production of chlorofluorocarbons was phased out, leading to a decrease in tropospheric chlorine beginning in 1993. The annual changes in ozone are discussed in more detail in the supplementary material on *Science* Online.

Note the substantial drop in total column ozone the year following most volcanic eruptions labelled by name in red. Ozone depletion is accompanied by decreasing temperatures in the lower stratosphere (purple line) mostly following the major explosive eruptions of Agung (1963), El Chichón (1982) and Pinatubo (1991) (*16, 17*).

In 1991, the major eruption of Mt. Pinatubo in the Philippines depleted ozone 6% but exploded 17 megatons of sulfur dioxide (*18*) into the lower stratosphere where it formed a sulfuric-acid aerosol approximately 15 to 25 km above Earth (*19*) that spread throughout the world over several months. The aerosol particles grew large enough to reflect and scatter sunlight, cooling Earth ~0.5°C for three years. The ozone layer was most depleted during late winter, causing warming over continents (*20*), but the globally distributed aerosols caused net cooling. Such cooling has been observed after all major explosive volcanic eruptions throughout human history. When such eruptions happen frequently – every decade or so – their cumulative effects can decrease ocean temperatures substantially (Fig. S3), ultimately ushering in an ice age.

But effusive basaltic volcanoes do not form aerosols in the stratosphere causing net warming as shown clearly from 11,750 to 9,350 years ago when thousands of basaltic lava flows erupted throughout much of Iceland (*21*) when the ocean was being warmed out of the last ice age (darkest red area, Fig. S2).

Every 22 million years, on average (*22*), massive eruptions of basaltic lava covered areas as large as the contiguous United States. Some of these events lasted for hundreds of thousands of years, extruding up to four million cubic kilometers of basaltic lava, contemporaneous with lethally hot temperatures, acidic oceans, major ozone depletion, increased rates of mutation, and major mass extinctions (*23-26*).

Climate throughout Earth's history appears controlled by the frequency of major explosive volcanic eruptions forming aerosols that cause cooling and the duration of effusive, basaltic volcanic eruptions causing ozone depletion and associated warming (Fig. 3). The relative proportion of these two types of volcanism is determined by plate tectonics processes that control the relative motion of tectonic plates. For example, 56.1 million years ago, global temperatures rose 6°C associated with voluminous basaltic eruptions during the initial opening of the Greenland-Norwegian Sea (*27, 28*).

20th Century Climate Change

Average global surface temperatures cooled (Fig. 4) following the major explosive eruptions of Tambora (1815), Krakatau (1883), Santa Maria (1902), and Novarupta/Katmai (1912). Then temperatures rose as smaller, more moderate and more effusive eruptions occurred once or twice per year through 1943 (*29*). A highly unusual sequence of seven small volcanic eruptions around the Pacific Ocean from 1931 through 1933 preceded the great "Dust Bowl" droughts and warming worst in 1934 and 1936.

Average temperatures were relatively constant from 1945 until 1970 (Figs. 4, 5). Then temperatures rose sharply from 1970 through 1998 (Fig. 5, red bars), contemporaneous with a substantial increase in chlorofluorocarbon gases (CFCs) manufactured for use as propellants in spray cans, as refrigerants, and as solvents. The green line shows total tropospheric chlorine (*14*), which tends to lead stratospheric chlorine by 3 to 5 years, estimated from the baseline scenario of the 1998 Scientific Assessment of Ozone Depletion (*30*). Production of CFCs increased rapidly after 1965, as did tropospheric chlorine (green line) and ozone depletion (black line). In 1974, scientists discovered that CFCs, when exposed to ultraviolet sunlight in very cold environments, can release chlorine atoms that destroy ozone in the lower stratosphere (*10*). Discovery of the ozone hole over Antarctica in 1984 (*15*) added urgency to negotiate the Montreal Protocol on Substances that Deplete the Ozone Layer. Under this protocol, emissions of CFCs began to decline by 1993, halting the increase in ozone depletion by 1996. Some of these very stable gases are expected to remain in the atmosphere until 2070. As long as ozone remains depleted, the ocean will continue to warm.

Global temperatures have remained relatively constant since 1998 (Figs. 4, 5). But record warm temperatures and drought in central and northeastern North America during 2012 and 2013 appear directly related in time and location to 15% ozone depletion measured over Toronto Canada: 3% due to CFCs, 6% due to the eruption of Eyjafjallajökull volcano in Iceland in 2010, and 6% due to the eruption of Grímsvötn volcano in Iceland in 2011 (Fig. S4).

Ozone depletion, relative to levels common in the 1960s, often exceeds 50% in the Antarctic "ozone hole" during late winter and early spring. But ozone depletion occurs throughout the world, exceeding 4% at all latitudes outside of the tropics. The greatest observed warming has been in regions with the greatest observed ozone depletion and has occurred during months when this depletion was greatest.

Ozone depletion caused by effusive volcanoes and stratospheric aerosols caused by explosive volcanoes (Fig. 3), provide mechanisms for global warming and cooling throughout geologic time. The rapid increase in CFC emissions by humans after 1965 and their decrease after 1992 appears to explain increased ozone depletion and global warming from 1970 to 1998 as well as the fact that both have remained relatively constant during the past 16 years. Concentrations of carbon dioxide in the atmosphere, meanwhile, have been rising steadily and the rate of increase has even increased since 1998 (Figs. 4, 5).

Ozone depletion caused by volcanoes and CFCs appears to explain qualitatively most observed global warming. It will take considerable data gathering and development of new models to quantify this relationship.

The Relative Effects of Ozone Depletion and Greenhouse Gases

Climate models currently estimate the total radiative forcing caused by changes in ozone concentrations as 0.35 W m^{-2} compared to 2.83 W m^{-2} for well-mixed greenhouse gases (*31*). But this metric only addresses the effects of ozone on atmospheric temperatures.

Climate models also assume that total energy contained in radiation is the sum of the energies absorbed along each spectral line and is thus proportional to bandwidth. But Planck showed in 1900 that energy in radiation is equal to frequency times the Planck constant. The major band of infrared energy absorbed by CO_2 has wavelengths from 13,100 to 17,300 nanometers and energy near 0.08 eV at each frequency. The narrow band of energy that reaches Earth when ozone is depleted has wavelengths from 300 to 330 nanometers but energies near 4 eV at each frequency, 48 times greater.

Energy is widely observed to be a function of frequency. Infrared radiation does not have enough energy (frequency) to penetrate glass or to cause the rods and cones in our eyes to oscillate. Visible light has enough energy to cause photosynthesis. Ultraviolet radiation has enough energy to damage DNA causing sunburn and mutations. It also has sufficient energy to dissociate oxygen and ozone. X-rays have enough energy to penetrate your body, but also to destroy DNA unless the amount (dosage) is kept very small.

The frequencies (colors) of radiation do not change over galactic distances except for Doppler effects and do not interact with each other. If they did, the colors of everything we see would be blurry. Thus the energy at each frequency is not shared with the energy at other frequencies and the energies are not additive (Fig. S5); each frequency (color) has its own energy and has an amount of that energy that we think of as intensity, brightness, or flux.

In matter, on the other hand, frequencies are initially determined by the normal modes of oscillation of each degree of freedom of each bond that holds atoms or molecules together. Energy, in this case, is shared through mechanical contact.

Max Planck (*1*) developed empirically an equation for the amount of radiation observed at each frequency emitted by a black body at thermal equilibrium as a function of its temperature (Fig. 6). Note that a warmer body always has more spectral radiance at every frequency than a cooler body and that the frequency of the peak in spectral radiance increases in both frequency and spectral radiance with increasing temperature (the dashed black line known as Wien's displacement law).

Peak spectral radiance can be thought of as the "color temperature" of radiation, the maximum temperature to which a black body could be raised when enough of that radiation was available. The color temperature is 288K for radiation from Earth (vertical green bar), 3300K for radiation from the filament of an incandescent light bulb, 5770K for radiation from the sun, and 16,500K for the band of ultraviolet-B energy reaching Earth when ozone is depleted (vertical violet bar). To increase the temperature of a black body, you must increase the color temperature. A body of matter can only be warmed by

5

absorbing radiation that has a higher color temperature than its own. Ultraviolet-B radiation penetrating to Earth when ozone is depleted (vertical violet bar) has 58 times the color temperature of Earth.

Trenberth et al. (*32, 33*) conclude that Earth radiates 396 W m^{-2} into the atmosphere and that greenhouse gases in the atmosphere radiate 333 W m^{-2} (84%) back to Earth, warming Earth (Fig. S6). Radiation from Earth cannot warm Earth because it has the same color temperature, the same frequency content. Greenhouse gases only absorb certain frequencies of terrestrial radiation and those frequencies greater than 16.93 terahertz, the frequency associated with the color temperature 288K, if radiated efficiently back to Earth, could conceivably warm Earth. The energy involved, however, is minimal compared to ultraviolet-B radiation.

Greenhouse gases are also thought to warm the atmosphere, decreasing the rate that heat can leave Earth. The rate that heat leaves Earth is proportional to the lapse rate, the decrease in temperature with increasing height from the bottom to the top of the troposphere. The lapse rate averages 6.4^{o}C/km ranging from 10°C/km in very dry air to 5.5^{o}C/km in very humid air. Water vapor is a greenhouse gas and clearly has an effect on the lapse rate. But as described by Fourier in 1822 (*34*), Earth's surface loses very little heat by radiation compared to the primary loss of heat by hot air rising and associated convection driving weather systems throughout the troposphere. We all lose heat more rapidly when the wind blows.

While Planck showed that radiant energy is proportional to frequency and therefore should be plotted on the x-axis as shown along the top of Fig. 6, he included energy as watts on the y-axis by including the Planck constant in the definition of spectral radiance. In 1900, most physicists were convinced that electromagnetic radiation propagates in a manner similar to waves in matter as defined by Maxwell's equations (*35*). The wave theory of light was widely accepted then and still is. But electromagnetic radiation in space, unlike waves in matter, shows a distinct difference between frequency and amount: frequency does not vary with distance while amount varies inversely with the square of the distance. Spectral radiance should be amount or flux without units of watts.

The color temperature of ultraviolet-B radiation is 16,500K, heating Earth's surface at 288K very efficiently, vaporizing water, causing major drought in some continental areas, major flooding where weather systems bring ocean air onto continents, and heating the oceans.

Total column ozone undergoes large day-to-day fluctuations of more than 50% primarily at mid- to polar-latitudes during winter and spring (*36*). Cyclic production and destruction of ozone generates heat regionally, affecting weather. An increase in the normal amount of ozone traps more ultraviolet-B radiation in the stratosphere, causing colder temperatures at the surface. Ozone depletion, on the other hand, causes surface warming, cooling the stratosphere. These fluctuations over areas of millions of square kilometers cool or warm tropospheric air and relate spatially to surface low-pressure and high-pressure areas and the paths of the jet-streams (*37*). Daily maps of ozone worldwide (*36*) may prove very useful in understanding weather.

What Actions Should We Take?

We humans have caused the world to warm ~0.6$^\mathrm{o}$C from 1970 to 1998. We have halted the human-caused increase in ozone depletion by reducing emissions of CFCs via the Montreal Protocol. We need to continue to strengthen the prohibition against manufacturing gases that deplete ozone and to seek ways to remove these gases from the atmosphere. As long as ozone remains depleted, the ocean will continue to absorb increased ultraviolet-B insolation. Earth's thermostat is being reset. The only natural way to lower the thermostat is through increased numbers of major explosive volcanic eruptions.

We also need to understand better exactly how volcanoes deplete ozone and what our options will be if the rates and types of global volcanism should suddenly change.

Increasing anthropogenic emissions of carbon dioxide and other greenhouse gases do not appear to influence global warming directly as currently assumed. Reducing these emissions is unlikely to reduce global warming, but may slow ocean acidification.

Rapid increases in pollutants such as black carbon formed by incomplete combustion, sulfur dioxide from burning fossil fuels, and ground-level ozone formed as a result of nitrogen oxides, volatile organic compounds, and other pollutants occurred 30 years prior to major warming (Fig. S7), suggesting that they do not have much effect on global warming other than absorbing some ultraviolet-B radiation. But these pollutants do have major deleterious effects on public health and many cause acid rain. Most developed countries have reduced pollution to relatively healthy levels, but improvements are still possible and of value. Developing countries rapidly increasing energy use, such as China and India, need to put major emphasis on reducing pollution for the health of their citizens and others living downwind. Concentrations of corrosive sulfate in acid rains that reach the western United States from Asia and from ships at sea approach and sometimes exceed US maximum allowable emission levels (*38*).

Our modern lifestyles depend heavily and increasingly on the availability of inexpensive energy. Sources of fossil fuels are limited. Currently, we waste more than 58% of the energy we produce for consumption (*39*). While much of this waste is inevitable, much can be conserved. Conserving energy not only makes good economic sense, but it also extends the long-term availability of fossil fuels.

The data and interpretations in this paper are described in much greater detail on the website ozonedepletiontheory.info.

References and Notes:

1. M. Planck, Entropie und temperatur strahlender wärme. *Ann. Phys.* **306**, 719 (1900).
2. S. Chapman, A theory of upper-atmospheric ozone. *Mem. Roy. Meteor. Soc.* **3**, 103 (1930).
3. M. Tedetti, R. Sempéré, Penetration of ultraviolet radiation in the marine environment. A review. *Photochem. Photobiol.* **82**, 389 (2006).
4. J. R. Herman, Global increase in UV irradiance during the past 30 years (1979–2008) estimated from satellite data. *J. Geophys. Res* **115**, D04203 (2010).
5. G. L. Manney *et al.*, Unprecedented Arctic ozone loss in 2011. *Nature* **478**, 469 (2011).
6. G. L. Hughes, S. S. Rao, T. S. Rao, Statistical analysis and time-series models for minimum/maximum temperatures in the Antarctic Peninsula. *Proc. Roy. Soc. London, Ser. A* **463**, 241 (2007).

7.   R. Mulvaney *et al.*, Recent Antarctic Peninsula warming relative to Holocene climate and ice-shelf history. *Nature* **489**, 141 (2012).

8.   D. H. Bromwich *et al.*, Central West Antarctica among the most rapidly warming regions on Earth. *Nature Geosci.* **6**, 139 (2013).

9.   R. von Glasow, Atmospheric chemistry in volcanic plumes. *Proc. Nat. Acad. Sci. U.S.A.* **107**, 6594 (2010).

10.   M. J. Molina, F. S. Rowland, Stratospheric sink for chlorofluoromethanes: Chlorine catalysed destruction of ozone. *Nature* **249**, 810 (1974).

11.   WOUDC, World Ozone and Ultraviolet Radiation Data Center, www.woudc.org/data_e.html (2014).

12.   J. Staehelin *et al.*, Total ozone series at Arosa (Switzerland): Homogenization and data comparison. *J. Geophys. Res.* **103**, 5827 (1998).

13.   A. Douglass *et al.*, Chapter 2: Stratospheric ozone and surface ultraviolet radiation, in *Scientific Assessment of Ozone Depletion: 2010,* C. A. Ennis, Ed. (World Meteorological Organization Global Ozone Research and Monitoring Project - Report No. 52, 2011) pp. 76.

14.   S. Solomon, Stratospheric ozone depletion: A review of concepts and history. *Rev. Geophys.* **37**, 275 (1999).

15.   J. C. Farman, B. G. Gardiner, J. D. Shanklin, Large losses of total O_3 in atmosphere reveal seasonal ClO_x/NO_x interaction. *Nature* **315**, 207 (1985).

16.   W. J. Randel, Variability and trends in stratospheric temperature and water vapor, in The Stratosphere: Dynamics, Transport and Chemistry. *Geophys. Monogr.* **190**, 123 (2010).

17.   D. W. J. Thompson, S. Solomon, Understanding recent stratospheric climate change. *J. Clim.* **22**, 1934 (2009).

18.   T. M. Gerlach, H. R. Westrich, R. B. Symonds, Preeruption vapor in magma of the climactic Mount Pinatubo eruption: Source of the giant stratospheric sulfur dioxide cloud, in *Fire and mud: Eruptions and lahars of Mount Pinatubo, Philippines,* C. G. Newhall, R. S. Punongbayan, Eds. (Philippine Institute of Volcanology and Seismology and University of Washington Press, 1996) pp. 415-433.

19.   S. Self, J.-X. Zhao, R. E. Holasek, R. C. Torres, A. J. King, The atmospheric impact of the 1991 Mount Pinatubo eruption, in *Fire and Mud: Eruptions and lahars of Mount Pinatubo, Philippines,* C. G. Newhall, R. S. Punongbayan, Eds. (Philippine Institute of Volcanology and Seismology and University of Washington Press, 1996) pp. 1089-1115.

20.   A. Robock, Pinatubo eruption: The climatic aftermath. *Science* **295**, 1242 (2002).

21.   J. M. Licciardi, M. D. Kurz, J. M. Curtice, Glacial and volcanic history of Icelandic table mountains from cosmogenic [3]He exposure ages. *Quat. Sci. Rev.* **26**, 1529 (2007).

22.   V. E. Courtillot, P. R. Renne, On the ages of flood basalt events. *C.R. Geosci.* **335**, 113 (2003).

23.   M. K. Reichow *et al.*, The timing and extent of the eruption of the Siberian Traps large igneous province: Implications for the end-Permian environmental crisis. *Earth Planet. Sci. Lett.* **277**, 9 (2009).

24.   H. Svensen *et al.*, Siberian gas venting and the end-Permian environmental crisis. *Earth Planet. Sci. Lett.* **277**, 490 (2009).

25.   M. M. Joachimski *et al.*, Climate warming in the latest Permian and the Permian–Triassic mass extinction. *Geology* **40**, 195 (2012).

26.   Y. Sun *et al.*, Lethally hot temperatures during the early triassic greenhouse. *Science* **338**, 366 (2012).

27.   M. Storey, R. Duncan, C. Tegner, Timing and duration of volcanism in the North Atlantic Igneous Province: Implications for geodynamics and links to the Iceland hotspot. *Chem. Geol.* **241**, 264 (2007).

28.   R. E. Zeebe, J. C. Zachos, G. R. Dickens, Carbon dioxide forcing alone insufficient to explain Palaeocene–Eocene Thermal Maximum warming. *Nature Geosci.* **2**, 576 (2009).

29.   Global Volcanism Program, Large Holocene eruptions, www.volcano.si.edu/world/largeeruptions.cfm (2014).

30. WMO, "Scientific Assessment of Ozone Depletion: 1998" (World Meteorological Organization, Global Ozone Research and Monitoring Project—Report No. 44, 1999).

31. G. Myhre *et al.*, Anthropogenic and natural radiative forcing, in *Climate Change 2013: The Physical Science Basis. Contribution of Working Group I to the Fifth Assessment Report of the Intergovernmental Panel on Climate Change* T. F. Stocker *et al.*, Eds. (Cambridge University Press, Cambridge, United Kingdom and New York, NY, USA, 2013) pp. 659-740.

32. K. E. Trenberth, J. T. Fasullo, J. Kiehl, Earth's global energy budget. *Bull. Am. Meteorol. Soc.* **90**, 311 (2009).

33. K. E. Trenberth, J. T. Fasullo, Tracking Earth's energy: From El Niño to global warming. *Surv. Geophys.* **33**, 413 (2012).

34. J. Fourier, *The Analytic Theory of Heat. archive.org/details/analyticaltheor00fourgoog* (1822).

35. J. C. Maxwell, A dynamical theory of the electromagnetic field. *Phil. Trans. R. Soc. London* **155**, 459 (1865).

36. Environment Canada, Archive of world ozone maps, exp-studies.tor.ec.gc.ca/clf2/e/ozoneworld.html (2014).

37. R. J. Reed, The role of vertical motion in ozone-weather relationship. *J. Meteorol.* **7**, 263 (1950).

38. J. Lin *et al.*, China's international trade and air pollution in the United States. *Proc. Nat. Acad. Sci.* **111**, (2014).

39. LLNL, Energy flow: Estimated energy use in 2012, flowcharts.llnl.gov (2014).

40. W. DeMore *et al.*, Chemical kinetics and photochemical data for use in stratospheric modeling, www.archive.org/details/nasa_techdoc_19970037557 (1997).

41. S. Levitus *et al.*, World ocean heat content and thermosteric sea level change (0-2000 m), 1955-2010. *Geophys. Res. Lett.* **39**, L10603 (2012).

42. Hadley Centre, HadAT: globally gridded radiosonde temperature anomalies from 1958 to present, www.metoffice.gov.uk/hadobs/hadat/images.html (2013).

43. Remote Sensing Systems, Description of MSU and AMSU data products, www.remss.com/msu/msu_data_description.html (2012).

44. NOAA, The global surface temperature is rising, www.ncdc.noaa.gov/indicators/ (2014).

45. J. Maeder, Total yearly ozone at Arosa, ftp://iaclin2.ethz.ch/pub_read/maeder/totozone_arosa_yearly (2013).

46. R. A. Kerr, Ozone takes a nose dive after the eruption of Mt. Pinatubo. *Science* **260**, 490 (1993).

47. C. G. Newhall, S. Self, The volcanic explosivity index (VEI) - An estimate of explosive magnitude for historical volcanism. *J. Geophys. Res.* **87**, 1231 (1982).

48. L. Siebert, T. Simkin, P. Kimberly, *Volcanoes of the World* (University of California Press, Berkeley, ed. 3, 2010), 551.

49. T. Druitt, Emplacement of the 18 May 1980 lateral blast deposit ENE of Mount St. Helens, Washington. *Bull. Volcanol.* **54**, 554 (1992).

50. P. L. Ward, Regional increases in total column ozone before volcanic eruptions, www.ozonedepletiontheory.info/pre-eruption.html (2014).

51. Wikipedia, Nuclear weapon testing, en.wikipedia.org/wiki/Nuclear_weapons_testing (2013).

52. H. S. Johnston, Expected short-term local effect of nuclear bombs on stratospheric ozone. *J. Geophys. Res.* **82**, 3119 (1977).

53. NOAA, Multivariate ENSO index (MEI), www.esrl.noaa.gov/psd/enso/mei/ (2013).

54. J. Gleason *et al.*, Record low global ozone in 1992. *Science* **260**, 523 (1993).

55. J. K. Angell, Estimated impact of Agung, El Chichón and Pinatubo volcanic eruptions on global and regional total ozone after adjustment for the QBO. *Geophys. Res. Lett.* **24**, 647 (1997).

56. J. Kerr, D. Wardle, D. Tarasick, Record low ozone values over Canada in early 1993. *Geophys. Res. Lett.* **20**, 1979 (1993).

57. M. De Mazière *et al.*, Quantitative evaluation of the post–Mount Pinatubo NO_2 reduction and recovery, based on 10 years of Fourier transform infrared and UV-visible spectroscopic measurements at Jungfraujoch. *J. Geophys. Res.* **103**, 10849 (1998).

58. P. Johnston, R. McKenzie, J. Keys, W. Matthews, Observations of depleted stratospheric NO_2 following the Pinatubo volcanic eruption. *Geophys. Res. Lett.* **19**, 211 (1992).

59.   M. T. Coffey, Observations of the impact of volcanic activity on stratospheric chemistry. *J. Geophys. Res.* **101**, 6767 (1996).

60.   J. K. Angell, Stratospheric warming due to Agung, El Chichón, and Pinatubo taking into account the quasi-biennial oscillation. *J. Geophys. Res.* **102**, 9479 (1997).

61.   J. G. Anderson, D. M. Wilmouth, J. B. Smith, D. S. Sayres, UV dosage levels in summer: Increased risk of ozone loss from convectively injected water vapor. *Science* **337**, 835 (2012).

62.   SPARC, The role of halogen chemistry in polar stratospheric ozone depletion, www.atmosp.physics.utoronto.ca/SPARC/HalogenChem_Final_20090213.pdf (2009).

63.   A. Tabazadeh, R. P. Turco, Stratospheric chlorine injection by volcanic eruptions: HCl scavenging and implications for ozone. *Science* **260**, 1082 (1993).

64.   J. Palais, H. Sigurdsson, Petrologic evidence of volatile emissions from major historic and pre-historic volcanic eruptions, in Understanding Climate Change. *Geophys. Monogr.* **52**, 31 (1989).

65.   C. Freda, D. Baker, P. Scarlato, Sulfur diffusion in basaltic melts. *Geochim. Cosmochim. Acta* **69**, 5061 (2005).

66.   A. Vance *et al.*, Ozone depletion in tropospheric volcanic plumes. *Geophys. Res. Lett.* **37**, L22802 (2010).

67.   U. Siegenthaler *et al.*, Stable carbon cycle-climate relationship during the Late Pleistocene. *Science* **310**, 1313 (Nov 25, 2005).

68.   D. Lüthi *et al.*, High-resolution carbon dioxide concentration record 650,000–800,000 years before present. *Nature* **453**, 379 (2008).

69.   H. Fischer, M. Wahlen, J. Smith, D. Mastroianni, B. Deck, Ice core records of atmospheric CO_2 around the last three Glacial terminations. *Science* **283**, 1712 (1999).

70.   E. Monnin *et al.*, Atmospheric CO_2 concentrations over the last glacial termination. *Science* **291**, 112 (Jan 5, 2001).

71.   N. Caillon *et al.*, Timing of atmospheric CO_2 and Antarctic temperature changes across termination III. *Science* **299**, 1728 (2003).

72.   L. Stott, A. Timmermann, R. Thunell, Southern Hemisphere and deep-sea warming led deglacial atmospheric CO_2 rise and tropical warming. *Science* **318**, 435 (2007).

73.   K. Tachikawa, L. Vidal, C. Sonzogni, E. Bard, Glacial/interglacial sea surface temperature changes in the Southwest Pacific ocean over the past 360 ka. *Quat. Sci. Rev.* **28**, 1160 (2009).

74.   J. B. Pedro, S. O. Rasmussen, T. D. van Ommen, Tightened constraints on the time-lag between Antarctic temperature and CO_2 during the last deglaciation. *Clim. Past* **8**, 1213 (2012).

75.   J. D. Shakun *et al.*, Global warming preceded by increasing carbon dioxide concentrations during the last deglaciation. *Nature* **484**, 49 (2012).

76.   F. Parrenin *et al.*, Synchronous change of atmospheric CO_2 and Antarctic temperature during the last deglacial warming. *Science* **339**, 1060 (2013).

77.   J. R. Petit *et al.*, Climate and atmospheric history of the past 420,000 years from the Vostok ice core, Antarctica. *Nature* **399**, 429 (1999).

78.   L. Siegenthaler, D. *et al.*, High-resolution carbon dioxide concentration record 650,000-800,000 years before present. *Nature* **453**, 379 (May 15, 2008).

79.   V. Fioletov, Ozone climatology, trends, and substances that control ozone. *Atmos. Ocean* **46**, 39 (2008).

80.   G. A. Zielinski, P. A. Mayewski, L. D. Meeker, S. Whitlow, M. Twickler, A 110,000-year record of explosive volcanism from the GISP2 (Greenland) ice core. *Quat. Res.* **45**, 109 (1996).

81.   J. W. C. White *et al.*, The climate signal in the stable isotopes of snow from Summit, Greenland: Results of comparisons with modern climate observations. *J. Geophys. Res.* **102**, 26425 (1997).

82.   J. M. Gregory, J. A. Lowe, S. F. B. Tett, Simulated global-mean sea level changes over the last half-millennium. *J. Clim.* **19**, 4576 (2006).

83.   Environment Canada, National climate data and information archive, www.climate.weatheroffice.gc.ca/climateData/dailydata_e.html?StationID=5097 (2013).

84.   S. J. Smith, R. Andres, E. Conception, J. Lurz, "Historical sulfur dioxide emissions 1850-2000: Methods and results" (2004).

85. S. J. Smith, H. Pitcher, T. M. L. Wigley, Global and regional anthropogenic sulfur dioxide emissions. *Global Planet. Change* **29**, 99 (2001).
86. HadCRUT3nh, HadCRUT3 northen hemisphere, www.cru.uea.ac.uk/cru/data/temperature/ (2014).
87. P. L. Ward, Climate trends, www.ozonedepletiontheory.info/trends.html (2014).
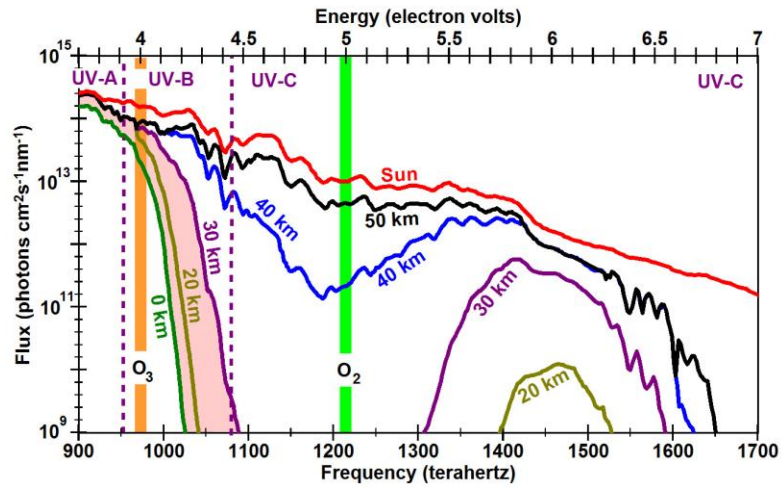
Fig. 1. When ozone is depleted in the ozone layer at altitudes of 15 to 35 km, more solar ultraviolet-B energy (red shading) reaches Earth, causing warming and drought. The red line shows the frequency (energy) distribution of solar radiation reaching the top of Earth's atmosphere (*40*). The black, blue, purple, olive, and green lines show how much of this radiation normally reaches lower altitudes (*40*).
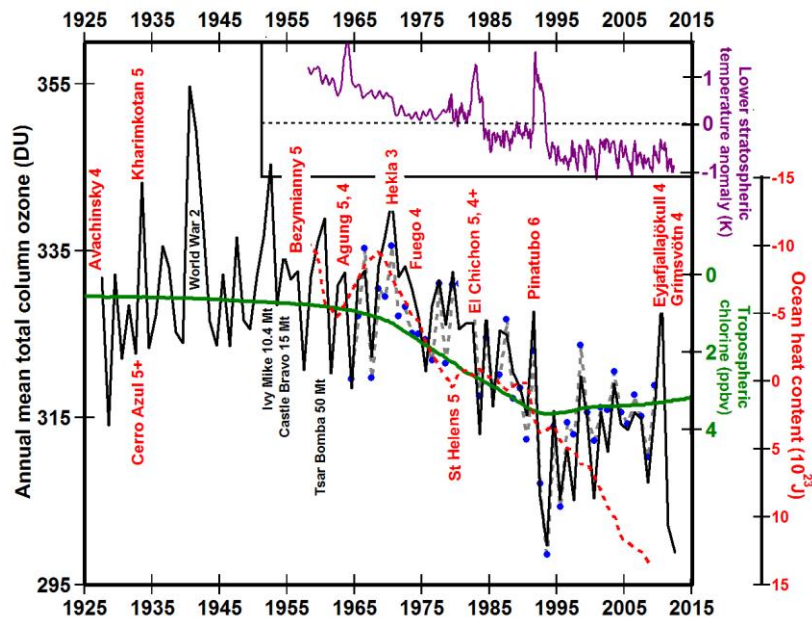
Fig. 2. Annual mean total column ozone (black line) peaks during years with major volcanic eruptions and then drops precipitously by more than twice as much during the following year, cooling the lower stratosphere (purple line) and warming the ocean (dashed red line, y-axis inverted) (*41*). The names of the erupting volcanoes and the Volcano Explosivity Index (VEI) for each large eruption are labelled in red (*29*). The green line shows annual mean tropospheric chlorine with the y-axis inverted (*14*). The purple line shows lower stratospheric temperature anomaly based on radiosonde data before 1979 (*42*) and satellite data since (*43*) smoothed with a seven-month centered running mean.
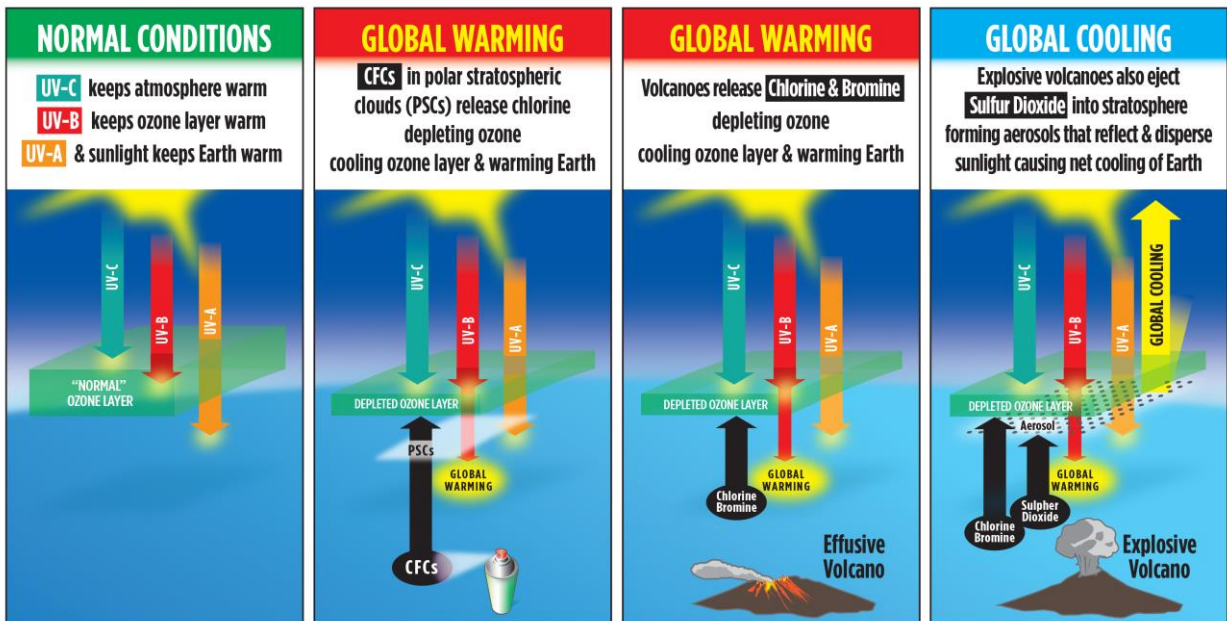
Fig. 3. **Global warming occurs when more ultraviolet-B sunlight than normal reaches the ocean because the ozone layer is depleted either by human-manufactured CFCs or by chlorine and bromine emitted by volcanic eruptions. Global cooling occurs when sulfuric-acid aerosols in the lower stratosphere reflect and disperse sunlight, decreasing the thermal energy reaching Earth. These aerosols are formed when sulfur dioxide gas is ejected into the stratosphere by large, explosive volcanoes.**
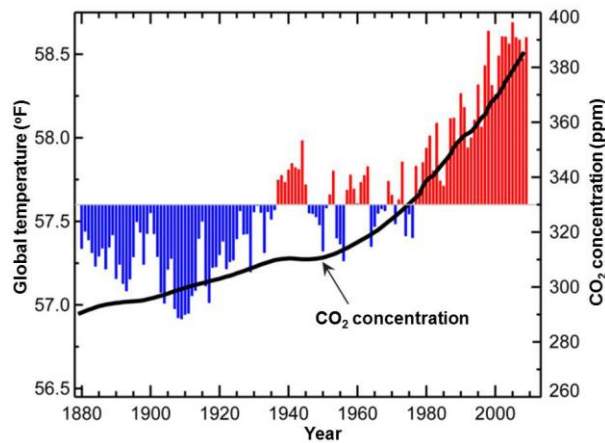

Fig. 4. Global temperatures rose primarily from 1910 to 1945 and from 1970 to 1998. Meanwhile carbon dioxide concentrations in the atmosphere have risen nearly continuously (*44*).

13
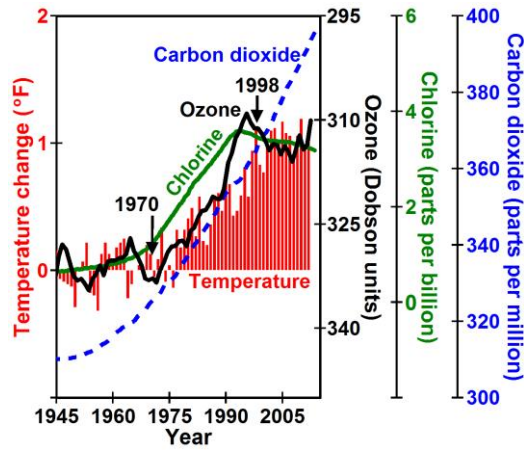
Fig. 5. Trends in temperature (red bars), tropospheric chlorine (green line) and ozone (black line) over the past 70 years are distinctly different from the trend in the concentration of carbon dioxide (blue dashed line). Increases of chlorine concentrations in the troposphere tend to precede by 3 to 5 years increases in the stratosphere that deplete ozone (*14*).
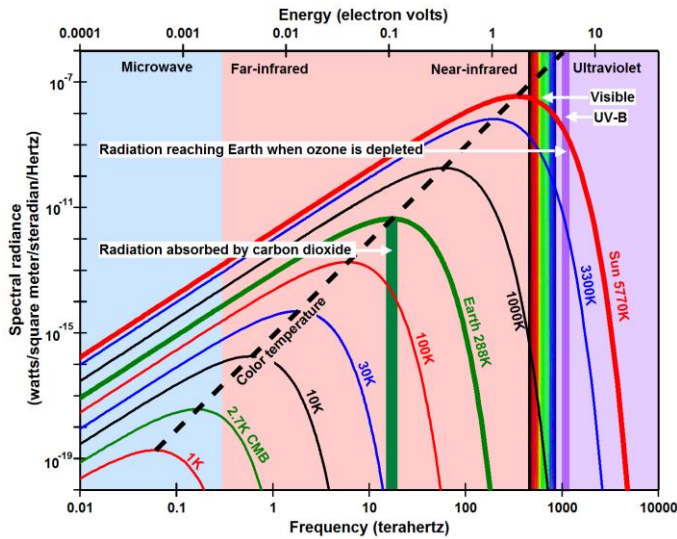

Fig. 6. Spectral radiance, the amount of radiation at each frequency, increases at every frequency and especially at higher frequencies as a body of matter warms. This distribution is approximated by Planck's law except units on the y-axis should not include watts because, for electromagnetic radiation, energy (watts) is equal to frequency times the Planck constant and is thus plotted on the x-axis shown at the top in electron volts.

14

Supplementary Materials:

Materials and Methods

An Extended Discussion of Figure 2

The lowest levels of annual mean total column ozone (*12, 45*) were observed in 1992 and 1993 following the 1991 eruption of Mt. Pinatubo (*46*), the largest explosive eruption since 1912, and in 2011 and 2012 following the eruptions of Eyjafjallajökull in 2010 and Grímsvötn in 2011, two of the larger effusive eruptions of the past century. The size of an explosive volcanic eruption is typically measured using the logarithmic Volcanic Explosivity Index (VEI) based primarily on the volume of tephra erupted and the maximum height of the eruption column (*47, 48*). The size of effusive volcanic eruptions is best measured using the volume of magma extruded. Volcanoes labelled in red (Fig. 2) include all very large explosive volcanic eruptions with VEI ≥5, some VEI 3 and 4 extrusive eruptions in Iceland, and two explosive VEI 4 eruptions from volcanoes elsewhere that typically included substantial lava flows. All volcanic eruptions shown were followed a year later by a substantial decrease in annual mean total column ozone except the 1980 eruption in Washington state of Mt. St. Helens, an unusual blast of steam triggered by a landslide on the intruding volcanic plug (*49*). Most other small volcanic eruptions since 1927 appear to cause similar changes in ozone, but the signal-to-noise ratios are too small to draw clear conclusions.

There is an increase in ozone the year of most of these eruptions compared to the previous year as discussed in more detail elsewhere (*50*). There are also large peaks in annual mean total column ozone during years containing the three largest atmospheric nuclear tests labelled in black with yield in megatons (Fig. 2) (*51, 52*). The largest short-term peak in ozone was in 1940 and 1941 during the major territorial conquests of World War II. Any causal relationship is unclear. There is also a peak in 1998 during one of the largest El Niños in history but no obvious peak in 1982 and 1983 during an El Niño with a comparably large multivariate ENSO index (*53*), although the latter observation may have been complicated by the eruption of El Chichón in 1982. The most consistent short-term changes in ozone in Fig. 2 are an apparent increase in ozone during the year of a volcanic eruption followed by a much larger depletion during the next few years.

Pinatubo erupted in the Philippines on 15 June 1991 (VEI 6) followed closely by the eruption of Cerro Hudson in southern Chile on 12 August 1991 (VEI 5+). Annual mean ozone increased 3.9% in 1991 primarily between February 19 and 26 (*50*). By 1993, annual mean ozone dropped 8.5% to 300 DU, the lowest level recorded by that time (*54, 55*). Total column ozone was 11 to 17% below preceding years throughout Canada with a peak loss of 30% at ~16 km (*56*). On average, total ozone decreased 8% in Europe, 5 to

6% in North America, Russia, and Asia but <2% in the tropics (*55*). Following the 1982 eruptions of El Chichón in Mexico (VEI 5 and 4+), total ozone similarly decreased 5% in Europe, 3% in North America and Russia and <1% in the tropics (*55*). Following the 1963 eruptions of Agung in Bali (VEI 5 and 4), total ozone fell 5% in Europe and Asia, 2% in North America, and <1% in the tropics (*55*).

An even larger ozone anomaly in 2010 is associated with the 100-times less-explosive basaltic effusive eruption of Eyjafjallajökull in Iceland (VEI 4). A slightly larger (VEI 4) eruption of Grímsvötn, 140 km northeast of Eyjafjallajökull, occurred in May 2011, compounding the amount of ozone depletion during 2011 and 2012. The amplitudes of these short-term ozone anomalies since 1990 are larger than the amplitudes of earlier volcanic anomalies before the global rise in tropospheric chlorine (green line, y-axis inverted). Similar anomalies appear associated with the eruption of Hekla in Iceland (1970, VEI 3).

Following the eruption of Pinatubo, the lower troposphere warmed up to $3^{\circ}C$ during the winter throughout the more northerly parts of the northern continents (*20*), the parts with greater depletion of ozone. Related major changes in atmospheric chemistry are well documented by a 45% drop in total column NO_2 above Switzerland beginning five months after the Pinatubo eruption and returning to normal with an e-folding time of two years (*57*), a 40% decrease in NO_2 column observed above New Zealand (*58*), and substantial increases in HNO_3 concentrations due to heterogeneous conversion of N_2O_5 (*59*).

The observed ozone depletion (black line, Fig. 2) was accompanied by cooling of the stratosphere (purple line) occurring mostly "as two downward 'steps' coincident with the cessation of transient warming after the major volcanic eruptions of El Chichón and Mount Pinatubo" (*17*) and a similar downward step following the 1963 eruptions of Agung volcano (*16*).

Ozone depletion following volcanic eruptions has traditionally been explained by new aerosols formed in the lower stratosphere providing substantial new surfaces for heterogeneous chemical reactions to form ozone-destroying chlorine at cold temperatures in a polar vortex (*60*). Yet water vapor (H_2O), the most voluminous gas erupted from volcanoes, is the primary source of OH radicals that catalytically destroy ozone in the stratosphere (*59, 61*). Volcanoes also erupt megatons of halogens (*59*), primarily chlorine and bromine (*62*), and only one halogen molecule can destroy >100,000 molecules of ozone (*10*). During explosive eruptions, many of these halogens appear to be removed immediately from the eruptive cloud in condensed supercooled water (*63*). But extrusive, basaltic eruptions such as Eyjafjallajökull and Grímsvötn do not form major eruption columns that remove halogens and that create aerosols in the stratosphere. They typically involve 10 to 100 times more volatiles per cubic kilometer of magma than explosive eruptions (*19, 64, 65*). Ozone depletion is substantial within the plumes of erupting volcanoes; detailed observations imply that "the most likely cause for the observed rapid and sustained O_3 loss to be catalytic reactions with halogen, mainly bromine, radicals" (*66*). Recent observations have shown that even the plumes of quiescently degassing volcanoes are chemically very active, containing halogens that modelling suggests cause ozone depletion (*9*). Between erupting many halogens and injecting large amounts of

water into the stratosphere (*61*), volcanoes appear to deplete ozone along many more chemical paths than attributed to anthropogenic chlorofluorocarbons.

Volcanic eruptions are typically followed a year later by ~6% depletion of ozone averaged throughout the year (Fig. 2). How do these short-term effects of volcanism compare to the longer-term effects of anthropogenic chlorofluorocarbons? The green line for chlorine is inverted and has been scaled so that the increase in anthropogenic tropospheric chlorine from 1965 to 1993 has approximately the same rate of change as the corresponding long-term decrease in ozone as expected by current theory. This visual fit suggests that depletion of ozone following the Pinatubo eruption (~20 DU) was twice as large as the depletion due to chlorofluorocarbons since 1960 (~10 DU) and that it takes more than a decade for ozone concentrations to return to pre-eruption levels.

In summary (Fig. 3), large, explosive volcanic eruptions are well known to form sulfuric acid aerosols in the lower stratosphere that reflect, scatter, and absorb solar radiation, causing cooling at Earth's surface of up to 0.6^{o}C over three years. These explosive eruptions also deplete ozone causing warming that lasts 3 to 5 times longer than the aerosols, but the cooling effects of the aerosol predominate during the first three years except in winter/spring over northern continents when ozone depletion is particularly strong. The much less explosive and much more numerous basaltic extrusive eruptions such as Eyjafjallajökull and Grímsvötn as well as quiescently degassing volcanoes (*9*) do not form substantial aerosols in the lower stratosphere so that warming due to ozone depletion predominates.

Increases in CO$_2$ Concentrations and Temperature at the End of Ice Ages
CO$_2$ concentrations have increased and decreased at nearly the same time as global temperatures during ice ages (*67, 68*). Many people see this as confirmation of greenhouse gas theory. But contemporaneity is not proof of cause. Most detailed studies suggest that CO$_2$ levels before the 20th century rose after temperature increased (*67, 69-74*). A few disagree (*75, 76*) pointing out that air is not trapped in snow until buried 50 to 120 meters, which can take hundreds of years in the Arctic and thousands of years in the Antarctic. The strong correlation between atmospheric temperatures and CO$_2$ concentrations going into and coming out of ice-age conditions (*67, 77, 78*) may primarily reflect the increase in solubility of CO$_2$ in a cooling ocean. From this perspective, CO$_2$ may be more a proxy for ocean temperature than a cause of increases in atmospheric temperatures.
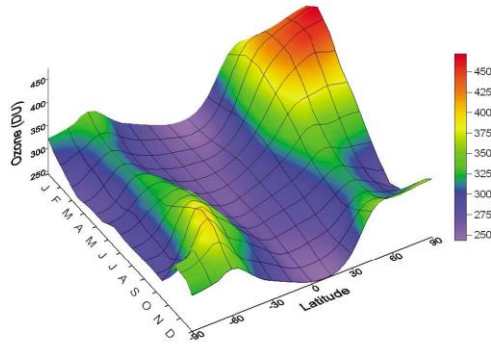
Fig. S1. Ozone accumulates during the winter in polar regions when the polar vortex is strongest. Ozone depletion is greatest in late winter and early spring. Zonal monthly mean total ozone in Dobson Units is shown as a function of latitude and month estimated from ground-based data for the period 1964 to 1980 (*79*). Excess ozone means more solar ultraviolet-B radiation is absorbed in the lower stratosphere, causing temperatures to become particularly cold near the ground.
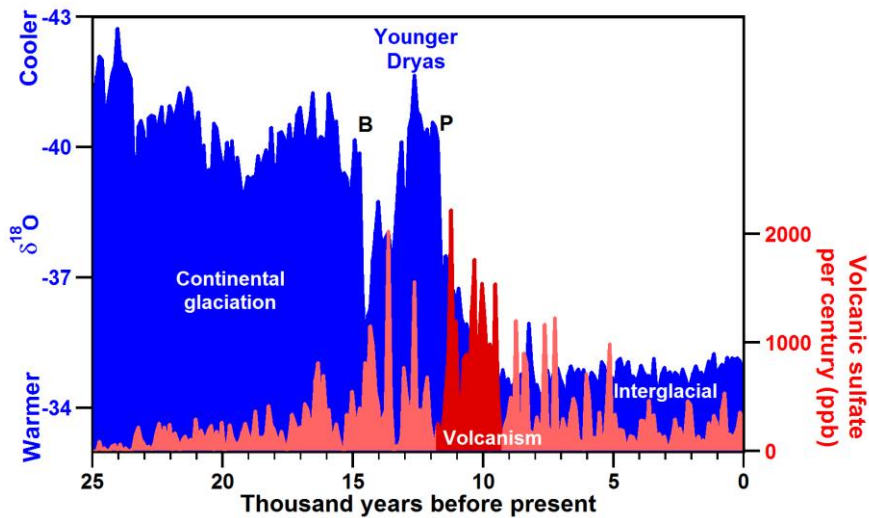

Fig. S2. Volcanic sulfate (red) measured in ice below Summit Greenland (*80*) shows a peak in volcanism between 11,750 and 9,350 years ago (darker red), the ages of many basaltic lavas in Iceland (*21*). This is the same time when the world warmed out of the last ice age according to an oxygen isotope proxy for local temperature (blue) measured in the same ice (*81*). B is the Bolling warming. P is the Preboreal warming.

18
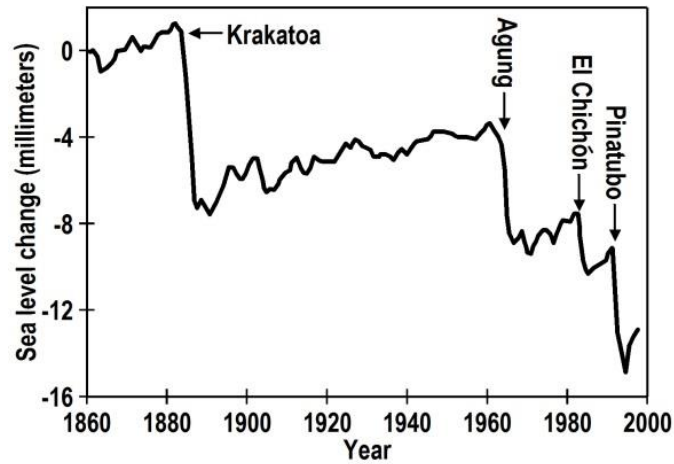
Fig. S3. Cumulative cooling of the ocean following several explosive volcanic eruptions modelled as a change in sea level. Sea-level change is often taken as a proxy for global temperature change (*82*).
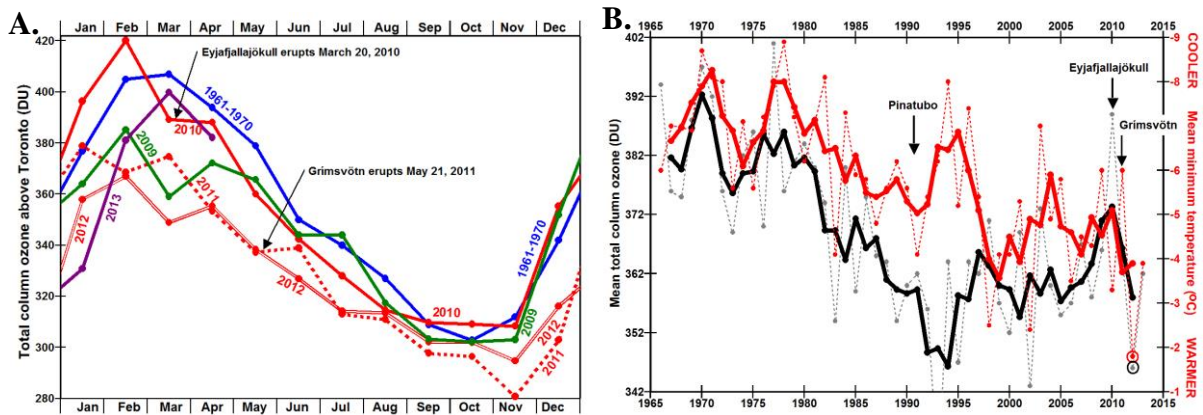

Fig. S4. Ozone concentrations reached a minimum in 2012 when temperatures reached a maximum. **A**, Total column ozone per month above Toronto, Canada, in November, 2011, was 12% below the average for Novembers in 1961 through 1970 (blue line) and has remained unusually low throughout 2012. **B**, When mean total column ozone measured during the months of December through April in Toronto Canada (black line) decreases, mean minimum temperature for the same months typically warms (red lines, y-axis inverted) except following the eruption of Pinatubo in 1991. Ozone data measured at Environment Canada and the University of Toronto (*11*). Temperature data measured at Toronto International Airport (*83*). The dashed lines show annual means; the solid lines are smoothed using a 3-point centered running mean.

19
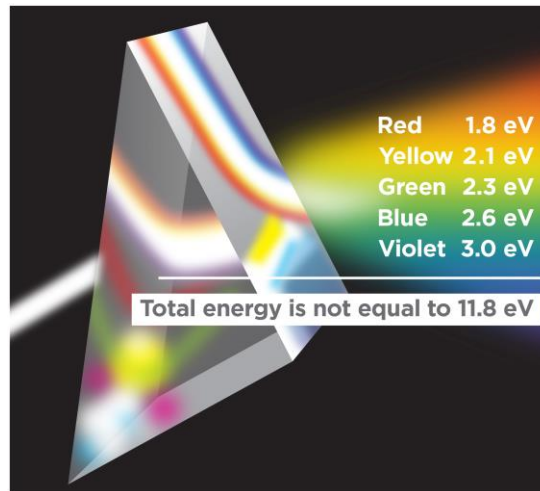
Fig. S5. A prism divides white light into its components. The total energy of the white light is not equal to the sum of the energies of each color in this rainbow as currently assumed when calculating the thermal effects of greenhouse gases. White light simply contains some of each of the colors of the rainbow and each color has a specific frequency and therefore a specific energy.
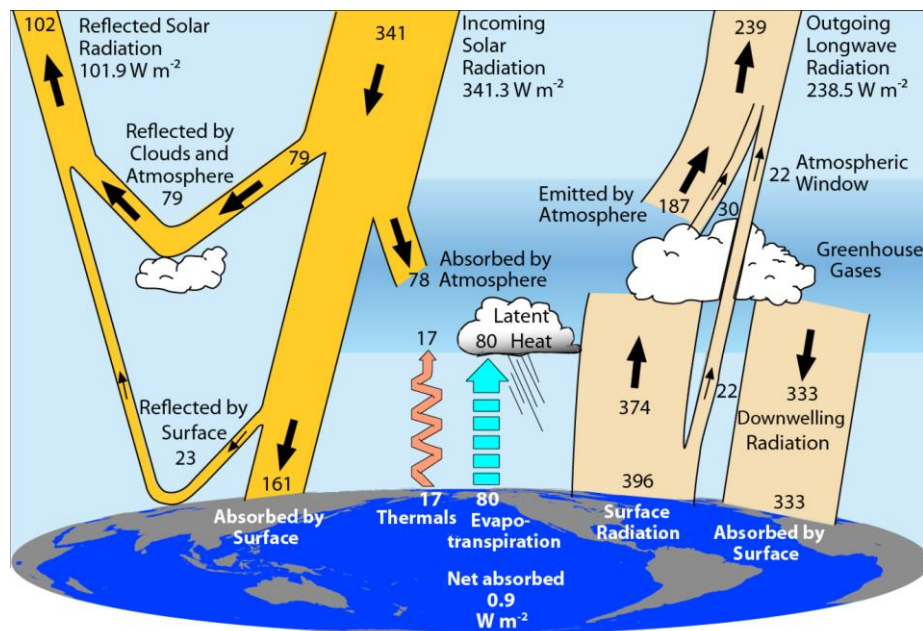

Fig S6 The global annual mean energy budget for Earth from 2000 to 2005 (W m^{-2}). The broad arrows indicate the schematic flow of energy in proportion to their importance. From Trenberth and Fasullo (*33*).
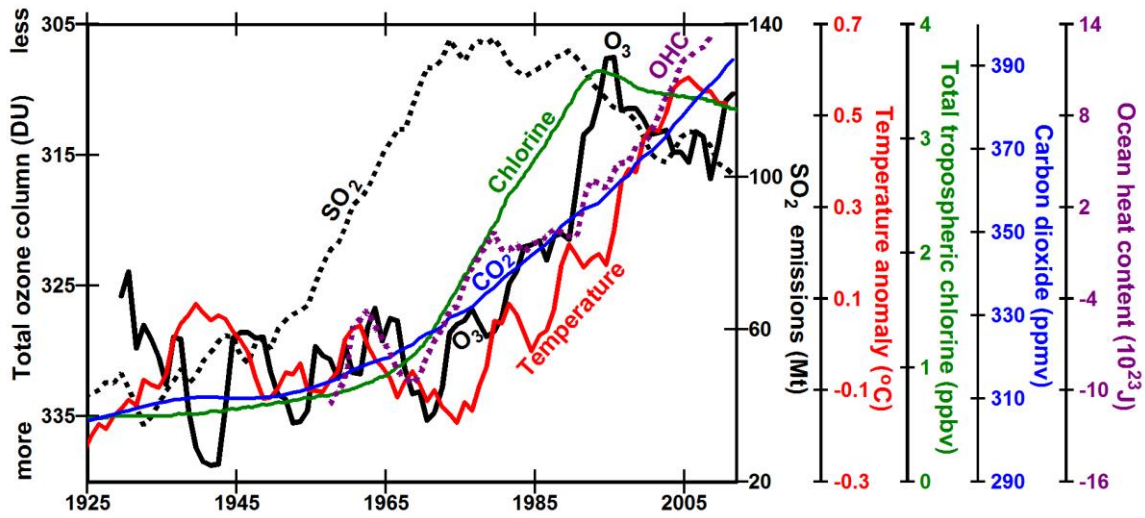
Fig. S7 Increased SO_2 pollution (dotted black line) (*84, 85*) does not appear to contribute to substantial global warming (red line) (*86*) until total column ozone decreased (black line, y-axis inverted) (*12*), most likely due to increasing tropospheric chlorine (green line) (*14*). Mean annual temperature anomaly in the Northern Hemisphere (red line) and ozone (black line) are smoothed with a centered 5 point running mean. OHC is ocean heat content (dotted purple line) (*41*). This figure and a related figure showing trends of NO_x, black carbon, methane, and surface solar radiation are described in detail elsewhere (*87*).